Temperature Cycling Analysis of Lead-Free Solder Joints in Electronic Packaging

Shan Li[a,*], Zhenyu Huang[a] and Jianfeng Wang[a], Shaowu Gao[b]
[a] Intel (Shanghai) Technology Development Ltd., Shanghai, China
[b] ABAQUS Shanghai Office, Shanghai, China

Abstract

Numerical simulations have found growing interests in evaluating interconnect reliability in electronic packaging, particularly for lead-free solder joints. To achieve good predictive capability, appropriate constitutive properties for the solder balls and a damage mechanism based life prediction model must be provided. In this paper, a simple published but efficient approach is adopted to predict life of SnAgCu joints subjected to temperature cycling. Specifically, the constitutive properties of the solder joints are described by the ABAQUS built-in Anand model, and the energy based Darveaux model is used to predict the fatigue life. The complete finite element model and its analysis are done in ABAQUS using its scripting interface. Finally a numerical example is presented to illustrate the procedures, and, hence, demonstrates the capability of ABAQUS in electronic packaging modeling.

1. Introduction

Solder joints have been widely used in the ball grid array (BGA) package to provide electrical and mechanical connections between the package and the PCB Board (see Fig. 1). However, a major concern with the solder joints is the effect of temperature cycling on the reliability of electronic packages since they are mainly subjected to cyclic power and thermal loadings during their service life. As the coefficients of thermal expansion (CTE) of the materials used in these packages are drastically different (2~3 ppm for die and 40~60 ppm for molding compound and die film), temperature variations create thermal mismatch resulting in solder joint stress during heating and cooling cycles. The damage caused by these stresses accumulates as the electronic assembly is subjected to thermal cycling, eventually leading to fatigue failures of solder joints. Thus, measuring thermal fatigue life of solder joint has always been an important factor when evaluating a package for a particular application.

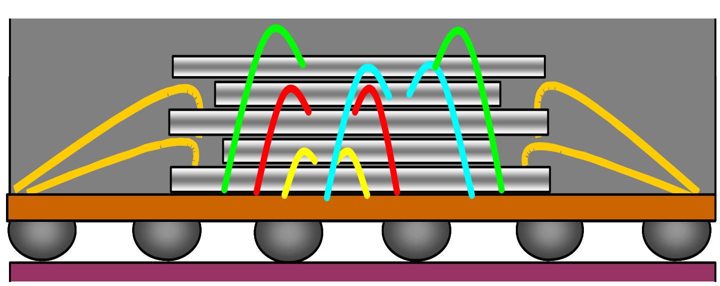

Fig.1 Schematic drawing of a ball grid array package

* Corresponding author. Flash Packaging Technology Development (FPTD-S), Intel (Shanghai) Technology Development Ltd., Phone: (021)387-33526. E-mail address: shan.li@intel.com (Shan Li).

Traditionally, the thermal fatigue life of solder joints is measured by performing temperature cycling tests which may take up to months. Even with accelerated life tests adopted, the task still remains formidable. With the maturity of numerical techniques and sophistication of computer resources, numerical simulations have rendered it possible to predict the life of solder joints without resorting to lengthy and costly tests. Compared with tests, numerical simulations are much cheaper and faster and can be readily used to aid designers in assessing risk at the early stage. Because of the benefits, now IC companies rely heavily on numerical simulation for reliability assessment of solder joints. However, to achieve good predictive capability, appropriate constitutive properties for the solder balls and a damage mechanism based life prediction model must be provided. Over the past decades, a number of models have been proposed to study lead- and lead free solder joints. Lau and Rice [1990] adopted an empirical elasto-plastic stress-strain relation for solder alloys. Wiese et al [2003] identified two mechanisms for steady state creep deformation of Sn4.0Ag0.5Cu (SAC405) solder and adopted a double power law to simulate climb controlled (low stress) and combined glide/climb (high stress) behavior. Darveaux [2000] used Anand visco-plasticity model [1985, 1989] to describe solder joints behavior at high temperatures and decomposed the failure into crack initiation and crack growth, both of which were approximated by power law.

The purpose of this work is to develop a modeling tool for new product thermal fatigue risk assessment as compared with old products benchmark values, therefore focus will be on aiming at "relative" life prediction rather than "absolute" values. The Anand Visco-plasticity model, which has been implemented in ABAQUS as a secondary creep law, is used in this study. Also since Darveaux's damage model [2000] has been verified by several researchers within 25% prediction accuracy, the previously published Data for both crack initiation and propagation are adopted to predict the thermal fatigue life for the lead-free sold joints. The complete finite element model and its analysis are done in ABAQUS using its scripting interfaces and global / local analysis technique is used to enhance the computation efficiency.

2. Constitutive properties

For most of metal alloys, creep usually occurs when homologous temperature, defined as the ratio of absolute temperature to the absolute melting temperature, is larger than 0.5. Since the melting temperatures of solder are around 200 °C, time-dependent creep phenomena are expected to dominate solder joint fatigue even at room temperature.

As shown in Fig. 2, creep deformation can be roughly divided into three regions:

Region I - Primary creep, which has a rapid rate initially and slows with time;
Region II - Secondary creep, which has a approximately uniform rate;
Region III - Tertiary creep, which has an accelerating creep rate and terminates by failure of material at time for rupture.

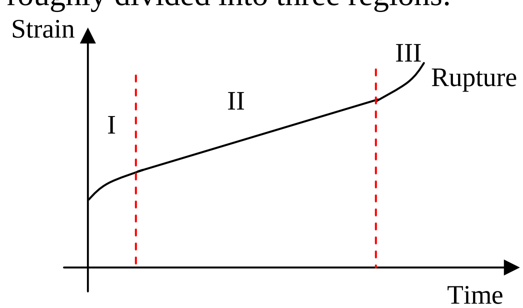

Fig.2 Strain Vs. Time Creep Behavior

In semi-conduct industries, the deformation kinetics of solder alloys is dominated by the steady state creep deformation due to their low melting point. Therefore, only the steady state creep behavior is considered in this study. The Anand model [1985, 1989], a viscoplasticity model that combines plasticity and creep deformation, is chosen to represent the secondary creep of solders. For ABAQUS Version 6.6, the Anand model is provided in the form of a built-in user material.

In Anand's model, the secondary creep is described by a flow equation:

$$\frac{d\varepsilon_p}{dt} = A\left[\sinh\left(\frac{\xi\sigma}{s}\right)\right]^{\frac{1}{m}} \exp\left(\frac{-Q}{kT}\right) \qquad (1)$$

where Q is the activation energy, k is the Boltzmann's constant, T is the absolute temperature, σ is the flow stress, A is the pre-exponential factor, m is the strain rate sensitivity, ξ is the multiplier of stress, and s is the deformation resistance stress built-in as a state variable and its evolution is given by the following three equations:

$$\frac{ds}{dt} = \left[h_0 (|B|)^a \frac{B}{|B|}\right] \frac{d\varepsilon_p}{dt} \qquad (2)$$

$$B = 1 - \frac{s}{s^*} \qquad (3)$$

$$s^* = \hat{s}\left[\frac{1}{A}\frac{d\varepsilon_p}{dt}\exp\left(\frac{Q}{kT}\right)\right]^n \qquad (4)$$

where h_0 is the hardening/softening constant, a is the strain rate sensitivity of hardening, $\hat{s}$ is a coefficient for deformation resistance saturation value, and n is the strain rate sensitivity for the saturation value. As can be seen in the above equations, there are nine material parameters in Anand model: A, Q, ξ, m, h_0, $\hat{s}$, n, a, and s_0 (initial value of the deformation resistance). The values for Sn4Ag0.5Cu (SAC405) solder are tabulated in Table 1[Reinikainen et al, 2005].

Parameter	s_o (MPa)	Q/k (K)	A (1/sec)	ξ	M	ho (MPa)	$\hat{s}$	n	a
Value	1.3	9000	500	7.1	0.3	5900	39.4	0.03	1.4

Table 1. Anand's constants for SAC405 solder [Reinikainen et al, 2005]

3. Life prediction models

To predict the fatigue life of the solder ball, a sophisticated model that incorporates damage should be provided. Among all of the strain and energy based methods, Darveaux's model is arguably the most popular one due to its documented correlation with the actual tests. In Darveaux's model [Darveaux, 2000], the failure can be split into two parts: the life associated with crack initiation and the life associated with crack growth. The number of cycles before crack initiation is given by:

$$N_0 = K_1 \Delta W^{K_2} \qquad (5)$$

And the crack growth rate per cycle is given by:

$$\frac{da}{dN} = K_3 \varDelta W^{K_4} \qquad (6)$$

Where $\varDelta W$ is inelastic energy density accumulated in a cycle, K_i (i=1..4) are material constants of the particular sold joints. Assuming uniform crack growth rate during crack propagation, the total cycles before failure are the summation of two failure mechanism:

$$N_a = N_0 + \frac{a}{da/dN} \qquad (7)$$

where a is the total distance the crack has to propagate until completed separating the solder joint from the board or the package. Here it can be assumed as the diameters of the interfaces near the package side or the board side. As observed in tests (see Fig. 3, Ghaffarian, 2000), thermal fatigue failures usually occur at the interfaces near either package side or board side. Therefore, a can be assumed as the solder diameters of the package-side or board-side interfaces.

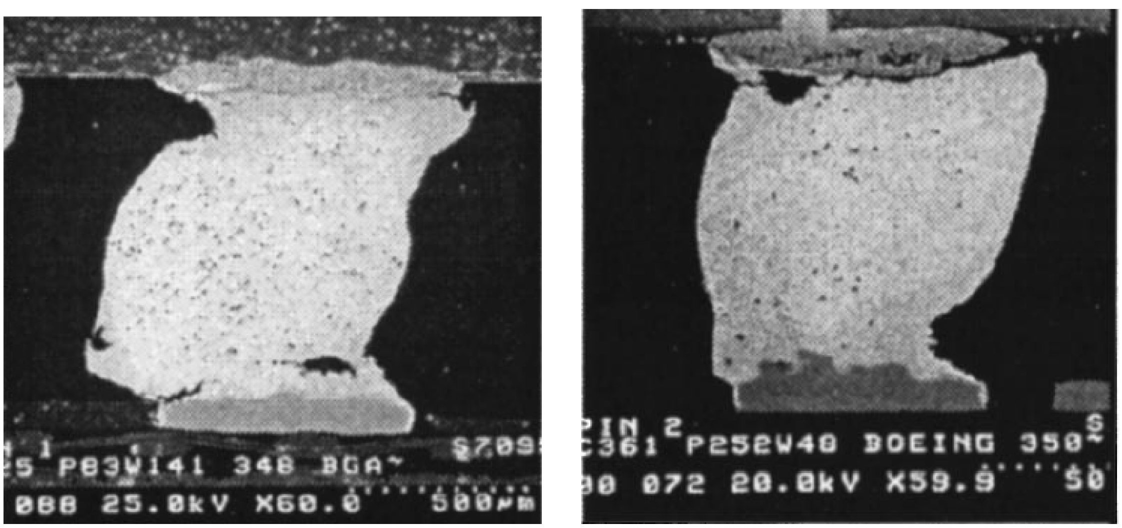

(a) (b)

Fig. 3 Common failure modes in thermal cycling tests (Ghaffarian, 2000)

The values for K_i for SAC405 joints are directly quoted from Darveaux [2000] and listed in Table 2.

Parameter	K_1 (cycles/MPa^{K_2})	K_2	K_3 (mm/cycles/MPa^{K_4})	K_4
Value	11.6	-1.52	7.71×10^{-9}	0.98

Table 2. Darveaux' life prediction constants for SAC405 solder [Darveaux, 2000]

4. Finite element implementation

To obtain the mechanical responses of the solder balls under thermal cycling, finite element code ABAQUS 6.6 [ABAQUS 6.6 manual] is used to perform the analysis.

Because of the large number of solder balls involved in a package and severe nonlinearity of Anand model, a single-step analysis of the full package with PCB board attached system would be computationally prohibitive. Therefore, it is necessary to provide a simplified model which can still yield an accurate, detailed solution for the solder. Since the solder balls have negligible effect on the deformation of the overall system, ABAQUS provides an ideal feature to fit this need: sub-modeling. This approach includes two subsequent analyses: a global analysis with a relatively coarse mesh used to simulate the whole 3D model of the PCB-solder-package assembly and a submodel analysis with a refined mesh to simulate the critical solder ball. These two analyses are linked together through transferring the time-dependent solutions saved in the global analysis to the relevant boundary nodes of the submodel. An outline of the procedures is shown schematically in Fig. 4. All of these modules, pre-process, solve, and post-process, are automated using ABAQUS python scripts. The four steps are described as follows:

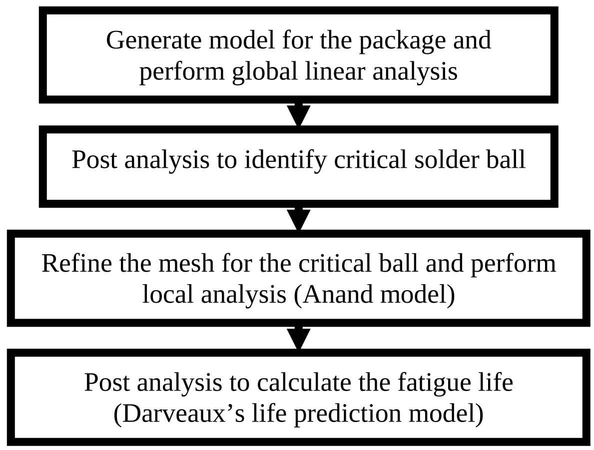

Fig. 4 Procedures for TC simulations

1. The global modeling. The purpose of global modeling is to identify the critical local ball and to provide driving boundary conditions for the subsequent submodeling analysis. Because of the symmetry, only a quarter of the PCB-solder-package assembly is modeled. Only linear elastic properties are assumed for package materials. Quadratic elements are used, with a typical mesh shown in Fig. 5a.

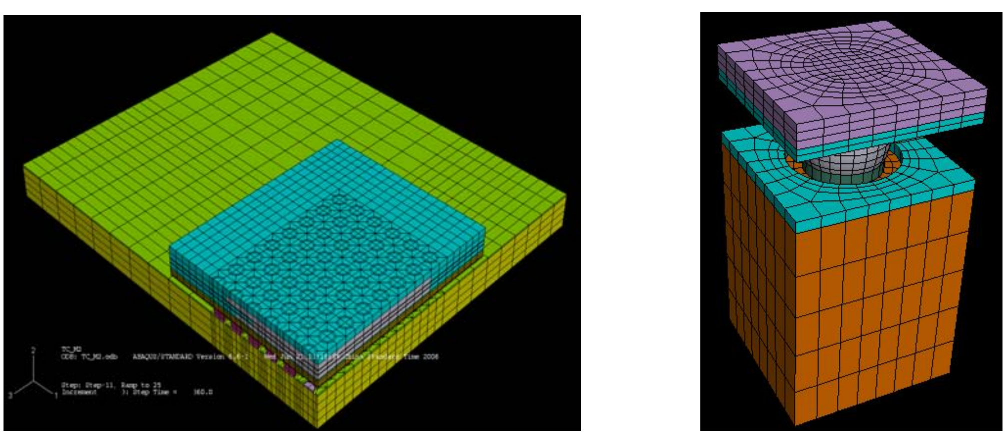

(a) (b)

Fig. 5 Finite element mesh for global (a) and local (b) models

2. Post global analysis. After the global analysis, an ABAQUS scripting interface is used to access the output database and to locate the solder ball with maximum Von-Misses stress. The position is then saved for next local modeling.

3. The submodeling. The local model includes only one critical solder joint with its location determined previously and part of the package and part of the board. The refined mesh is shown in Fig. 5b. The constitutive properties of the solder ball are captured by the Anand model. The driving boundary conditions are based on interpolation of the global solution around the vicinities of the critical solder ball.

4. Post local analysis. In this step, Darveaux' model is implemented to calculate the fatigue life of the solder ball. The accumulated creep energy density per cycle needs to be extract from the output database. To reduce stress concentration issues, volume-averaged energy density, ΔW_{ave}, is used which is given by:

$$\Delta W_{ave} = \frac{\sum dW_i V_i}{\sum V_i} \quad (8)$$

where dW_i and V_i are the incremental creep energy density per cycle and the volume associated with element i, respectively. The volume used to calculate the averaged energy is chosen as two 25 micron thick layers of solder elements near package and board sides.

5. Numerical examples

Numerical examples are provided here to illustrate the methodology described above. Two new ballouts, 110 and 116 balls, are considered here, as compared with the old product (95 balls). The layouts for the solder ball are shown in Fig. 6, respectively. To evaluate the reliability, a 3 stacked-die package is chosen with the dimensions tabulated in Table 3.

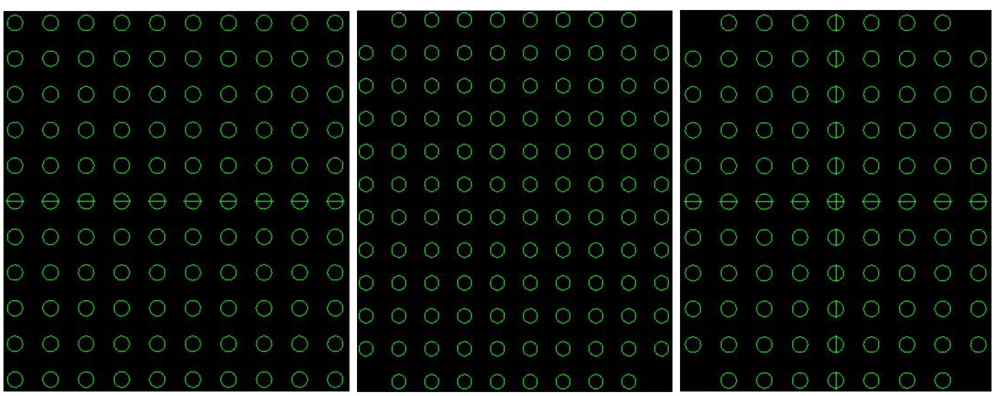

(a) (b) (c)

Fig. 6 Ballout for (a) 110, (b) 116, and (c) 95 balls

Package Size	Die Size	Mold Cap Thk	Sub Thk	Pitch	Ball Dia	Ball Height	Pad Type	Pad Size
9 x 10	6 x 8.2 x 0.125 5 x 8.5 x 0.125 7 x 8 x 0.125	0.65	0.2	0.8	0.4	0.25	SMD	0.45

Table 3 Dimensions (in mm) for the packages used in reliability evaluation

The temperature profile used in the study is shown in Fig. 7. The thermal cycle is from –40°C to 125 °C, with a temperature ramp rate of 11 °C/min ramp rate for 15 min. The dwell time at the low temperature and high temperature are both 15 min and the period is 1 h per cycle. Three cycles are simulated in both the global and local analyses.

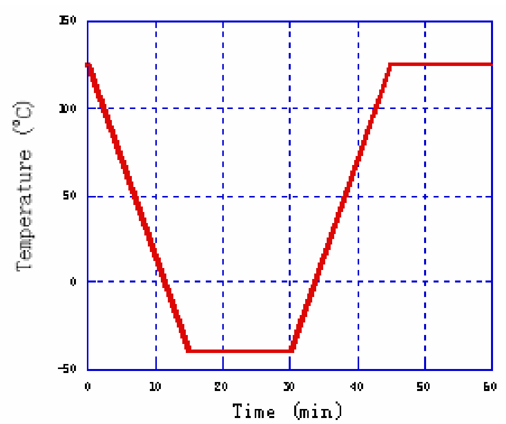

Fig. 7 Temperature profile used in FEM calculations

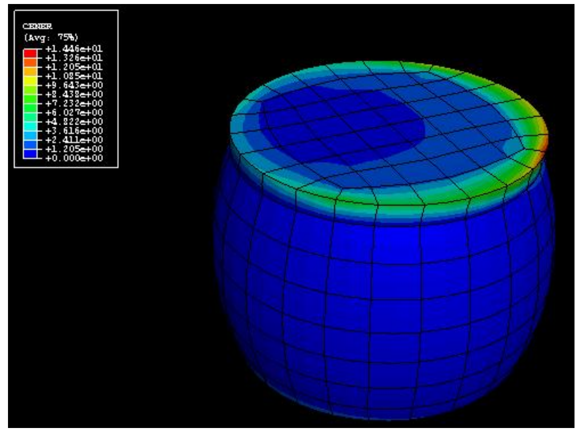

Fig. 8 Contour plot of creep strain density

Fig. 8 shows the contour plot of creep strain density for the critical solder ball at the end of a cycle. As can be seen, the maximum density occurs near the package side, which is consistent with the experimental observations (see Fig. 3). The correctly predicted failure location also provides justification for the choice of control volumes for averaged density calculations. Figs. 9 show the accumulated creep strain density near the package and board sides per cycle for three cycles for ballout a, b and c, respectively. As can be seen, significant portion of the accumulated strain density is gained during ramp stages while the increment during dwell is negligible. For all of these three ballouts, creep strain density clearly shows asymptote after the 2nd cycle, but it has not yet quite saturated. Hence the accumulated strain densities near the package side after the 3rd cycle are used for fatigue life evaluation in Eqs. 5-7. The predicted failure cycles for ballout 110 and 105 are roughly the same (449 cycles for 110 balls and 452 cycles for 105 balls), but both of them are marginal worse than the 116 balls (476)

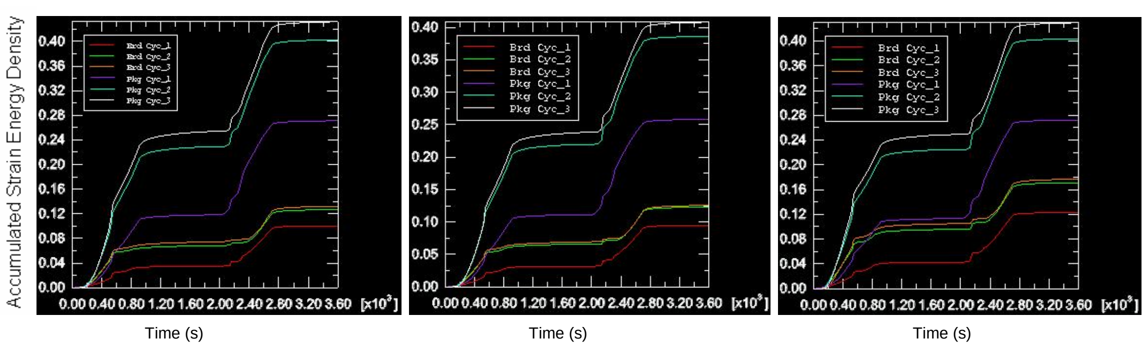

(a) (b) (c)

Fig. 9 Accumulated creep strain energy density per cycle for (a) 110, (b) 116, and (c) 95 balls

6. Conclusion

In this paper, Darveaux' model is implemented to study the thermal fatigue life of solder joints in BGA packages. Specifically, the Anand model, an ABAQUS built-in viscoplasticity model, is applied to represent the creep behavior for SAC405 solders. Global/local methodology is adopted to enhance computation efficiency. ABAQUS python scripting interfaces are used to generate the geometry mesh, perform analysis, and conduct post processing. The highly automated module provides a powerful tool for solder joint reliability analysis. Finally as a numerical example for capability demonstration, the implemented methodology is successfully applied to evaluate the temperature cycling reliability of three ballout designs.

7. Reference

ABAQUS manual version 6.6

Anand, L., "Constitutive Equations for Hot-Working of Metals," International Journal of Plasticity, Vol. 1, pp. 213-231, 1985.

Brown, S.B., K.H. Kim, and L. Anand, "An Internal Variable Constitutive Model for Hot Working of Metals," International Journal of Plasticity, Vol. 5, pp. 95-130, 1989.

Darveaux, R., "Effect of simulation methodology on solder joint crack growth correlation," in Proc. 50th Electronic Components and Technology Conf., May 2000, pp. 1048–1058.

Ghaffarian, Reza, "Accelerated Thermal Cycling and Failure Mechanisms for BGA and CSP Assemblies," *Journal of Electronic Packaging*, 2000, Volume 122, Issue 4, pp. 335-340.

Lau, J., and J. R. Rice, ''Thermal Stress/Strain Analyses of Ceramic Quad Flat Pack Packages and Interconnections,'' Proc. Elect. Components and Technology 40th Conf., Las Vegas, Nevada, 1990, Vol. 1, pp. 824–834.

Reinikainen, T.O., P. Marjadi, and J.K. Kivilahti, "Deformation Characteristics and Microstructural Evolution of SnAgCu Solder Joints," *EuroSIME 6th International Conference*, Germany, Apr. 2005, pp. 91-98.

Wiese, S., et al, "Microstructural Dependendence of Constitutive Properties of Eutectic SnAg and SnAgCu Solders," *53rd ECTC* ,2003, pp. 197-206.